



# Revisiting horizontal connectivity rules in V1: from like-to-like towards like-to-all

Frédéric Chavane, Laurent Perrinet, James Rankin

## ► To cite this version:

Frédéric Chavane, Laurent Perrinet, James Rankin. Revisiting horizontal connectivity rules in V1: from like-to-like towards like-to-all. *Brain Structure and Function*, 2022, 10.1007/s00429-022-02455-4 . hal-03572602

**HAL Id: hal-03572602**

**<https://hal.science/hal-03572602>**

Submitted on 15 Mar 2022

**HAL** is a multi-disciplinary open access archive for the deposit and dissemination of scientific research documents, whether they are published or not. The documents may come from teaching and research institutions in France or abroad, or from public or private research centers.

L'archive ouverte pluridisciplinaire **HAL**, est destinée au dépôt et à la diffusion de documents scientifiques de niveau recherche, publiés ou non, émanant des établissements d'enseignement et de recherche français ou étrangers, des laboratoires publics ou privés.

# Revisiting horizontal connectivity rules in V1: from like-to-like towards like-to-all

Chavane F<sup>1\*</sup>, Perrinet L<sup>1</sup>, Rankin J<sup>2</sup>,

<sup>1</sup> Institut de Neurosciences de la Timone (INT), CNRS and Aix-Marseille Université, UMR 7289, Campus Santé Timone, 27 boulevard Jean Moulin, Marseille 13005, France

<sup>2</sup> Department of Mathematics, College of Engineering, Mathematics & Physical Sciences, University of Exeter, Exeter EX4 4QJ, United Kingdom;

\* correspondence to FC, [frederic.chavane@univ-amu.fr](mailto:frederic.chavane@univ-amu.fr)

## Abstract

Horizontal connections in the primary visual cortex of carnivores, ungulates and primates organise on a near-regular lattice. Given the similar length-scale for the regularity found in cortical orientation maps, the currently accepted theoretical standpoint is that these maps are underpinned by a like-to-like connectivity rule: horizontal axons connect preferentially to neurons with similar preferred orientation. However, there is reason to doubt the rule's explanatory power, since a growing number of quantitative studies show that the like-to-like connectivity preference and bias are mostly observed at short-range scale, are highly variable on a neuron-to-neuron level and also depend on the origin of the presynaptic neuron. Despite the wide availability of published data to this effect, the accepted model of visual processing has never been revised. We review three lines of independent evidence supporting a much-needed revision of the like-to-like connectivity rule, ranging from anatomy to population functional measures, to computational models and theoretical approaches. We advocate an alternative, distance-dependent connectivity rule that is consistent with new structural and functional evidence: **from like-to-like bias at short horizontal distance to like-to-all at long horizontal distance**. This generic rule accounts for the observed high heterogeneity in interactions between the orientation and retinotopic domains, that we argue is necessary to process non-trivial stimuli in a task-dependent manner.

## INTRODUCTION

Retinotopy and orientation are two of the main features processed and topographically organized into maps in primary visual cortex (V1) of carnivores, ungulates and primates. Anatomical connections between neurons separated on the cortical sheet, through the so-called *intrinsic, intra-cortical* or *horizontal* axons have a crucial theoretical importance for understanding the computational operations that V1 can perform. Indeed, these axons connect different points in the retinotopic and orientation maps and thereby generate a set of possible topological interactions within a multidimensional representation of space, orientation and time. It is therefore critical to characterize structural horizontal interactions in order to understand their functional relevance. The vast majority of presynaptic contacts in cortex originate from neurons located in the same area as the postsynaptic target (>80% in macaque V1, (Markov et al. 2011), thus forming an intra-cortical network. In the primary visual cortex, the feedforward thalamocortical inputs drive the cortical network, which in turn strongly shapes the evoked response through major excitatory and inhibitory recurrent circuits within the column (Douglas et al. 1991), a canonical circuit that constitutes nearly  $\frac{2}{3}$  of intra-cortical connectivity (Markov et al. 2011). The rest of the intra-cortical network connects neurons in adjacent columns separated laterally over distances up to several millimeters, the so-called horizontal network. Early anatomical observations reported that the horizontal connectivity of carnivores, ungulates and primates is spatially distributed into regular clusters (Fig. 1A, (Braitenberg 1962; Fisksen et al. 1975; Creutzfeldt et al. 1977; Gilbert and Wiesel 1979; Rockland et al. 1982) forming a radially projecting pattern that resembles a daisy's petals (Douglas and Martin 2004). Since orientation maps are also regular with comparable spatial frequency, the currently accepted theoretical standpoint is that these maps are underpinned by a **like-to-like connectivity rule**: cortical columns are connected by horizontal connections only if they share similar orientation preference (Fig. 1A), an hypothesis originally put forward by Mitchison & Crick (Mitchison and Crick 1982). Correlative studies, comparing bouton labelling with autoradiography, or with optical imaging maps, qualitatively supported the like-to-like rule (Gilbert and Wiesel 1989). Later quantitative anatomical combined with optical imaging studies confirmed the existence of an orientation preference bias (Fig. 1B, in the range of 1.5-2 times greater than chance, Bosking et al. 1997, Kisvárdy 1997; Schmidt et al. 1997; Malach et al., 1993, Rochefort et al., 2009), with high cell-to-cell variability. Probably due to its simplicity and its elegant topological implications, the highlighted iso-orientation biases have led to a general acceptance of the hypothesis of a simplified and unique like-to-like connectivity. One consequence is that theoretical and computational models have implemented it as a strict rule, not as a bias (e.g. (Bressloff et al. 2001; Raizada and Grossberg 2003; Rangan et al. 2005; Sarti et al. 2008; Baker and Cowan 2009; Kaschube et al 2010; Rubin et al. 2015; Carroll and Bressloff 2016). However, we believe such an over-simplified schema may impair the development of our theoretical understanding of the primary visual cortex function.

Actually, there are reasons to doubt the explanatory power of a global and strict like-to-like connectivity rule. First, a growing number of quantitative studies show that there is a wide variety of connectivity biases (like-to-like bias, no bias, like-to-unlike bias) depending on cell type (Fig. 1C, excitatory vs inhibitory neurons, see Kisvárdy et al. 1994; Buzás et al. 2001),

layer origin (Fig. 1D, no bias in layer 4 or layer 6, see Yousef et al. 1999; Karube and Kisvarday 2010; Karube et al. 2017), and position in the orientation map (Yousef et al. 2001, iso-orientation domain vs pinwheels). Second, the effect is mostly observed at short-range where most of the connectivity arises (<1-1.5mm), but connections can connect neurons over distances of a few millimeters. The rare analyses over larger cortical distances (more difficult because far fewer boutons are present) showed a global tendency for the iso-orientation bias to reduce with distance (Fig. 1E) due to wider selectivity or deviation from the iso-orientation bias, as observed in Buzás et al. (2006, fig8C), Kisvarday et al (1997, Fig9 - area 17) and Bosking et al (1997, Fig 5); however, see a counter example for area 18 in Kisvarday et al (1997, Fig10 – area 18). As a consequence, the effective functional selectivity of horizontal axons beyond the short-range distance is not very clear. Lastly, the functional impact of the structural organisation, as described by anatomy, is far from being trivial to predict. Indeed, any visual stimulation will activate a neuronal mass encompassing all layers, both excitatory and inhibitory neurons and at least a full hypercolumn composed of pinwheels and iso-orientation domains (see Fig1D in Chavane et al 2011). Furthermore, not only neurons with preferred orientation matching the orientation of the stimulus will be significantly activated, but a distribution of neurons with say, +/-15 deg around the stimulus orientation. The intra-cortical horizontal network triggered by this functionally activated neuronal mass will forcibly contact a diversity of orientation tuned neurons (ranging from an iso-orientation, Fig. 1F, to an omni-orientation interaction, Fig. 1G) with an overall net effect beyond short-range distance that is particularly difficult to predict.

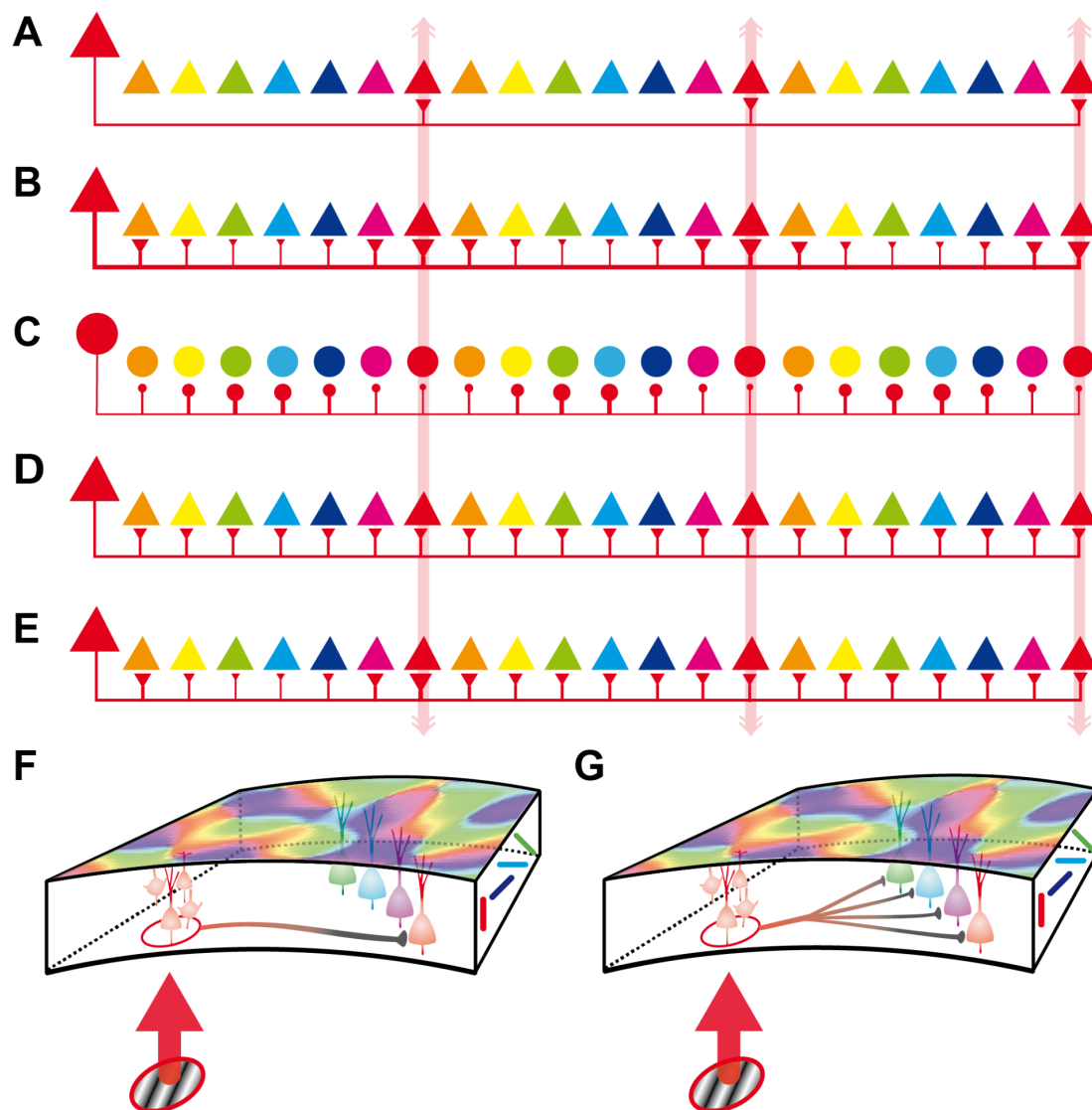


**Fig. 1: Illustration of different connectivity rules from literature and possible outcomes for functional activation.** In A-E the local neuron (large on left) connects to neighbours in a radially approximated schema spanning outwards over three hypercolumns (where the same preference is encountered, as indicated by the vertical arrows). Colors indicate the orientation preference of neurons. **(A)** Strict like-to-like connectivity (extends to long distances). **(B)** Modulated like-to-like bias (extends to long distances). **(C)** Like-to-unlike bias as exhibited by inhibitory interneuron. **(D)** Like-to-all as exhibited by neurons in layer 4 and 6. **(E)** Like-to-like bias that reduces with distance resulting in like-to-all at distances beyond adjacent hypercolumns. **(F-G)** Two extremes hypothesis for the net outcome of functionally driven connectivity rule at long-range distance. In response to a local oriented stimulus, all neurons that have a receptive field in overlap with the stimulus will be activated, for excitatory and inhibitory neurons, different lamina and positions in the orientation map. Such functional activation can lead either to a strict iso-orientation activation of neighboring neurons through the horizontal network (like-to-like rule, F) or omni-orientation activation (like-to-all rule, G).

In this review, we present a body of recent evidence from anatomy, physiology and computational modeling, leading to the conclusion that horizontal interactions do not forcibly conform with a like-to-like orientation preference. In the last decade, structural (Hunt et al. 2011; Martin et al. 2014, see Kisvarday 2016 for review), and functional (Chavane et al. 2011; Huang et al. 2014) studies have shown that the rule is not valid for long-distance connections. Chavane et al (2011) proposed revisiting the connectivity rule as a function of horizontal distance: from like-to-like at short distance towards like-to-all and long distances (Fig. 1E; see discussion in (Alonso and Kremkow 2014a, b). In their computational modelling study, (Rankin and Chavane 2017) show that this behavior is in fact to be expected based on the anatomical observations made by Buzas et al (2006). The functional implications of such evidence is further discussed in the framework of natural scenes analysis (Perrinet and Bednar 2015; Boutin et al. 2021). In light of converging evidence from a range of approaches, this review argues for a timely, in-depth revision of V1 horizontal connectivity rules. Revisiting this textbook mindset is an important prerequisite to better understand the relationship between structure and function in the visual cortex.

## NEW PHYSIOLOGICAL EVIDENCE

### *Neuronal population activity measures*

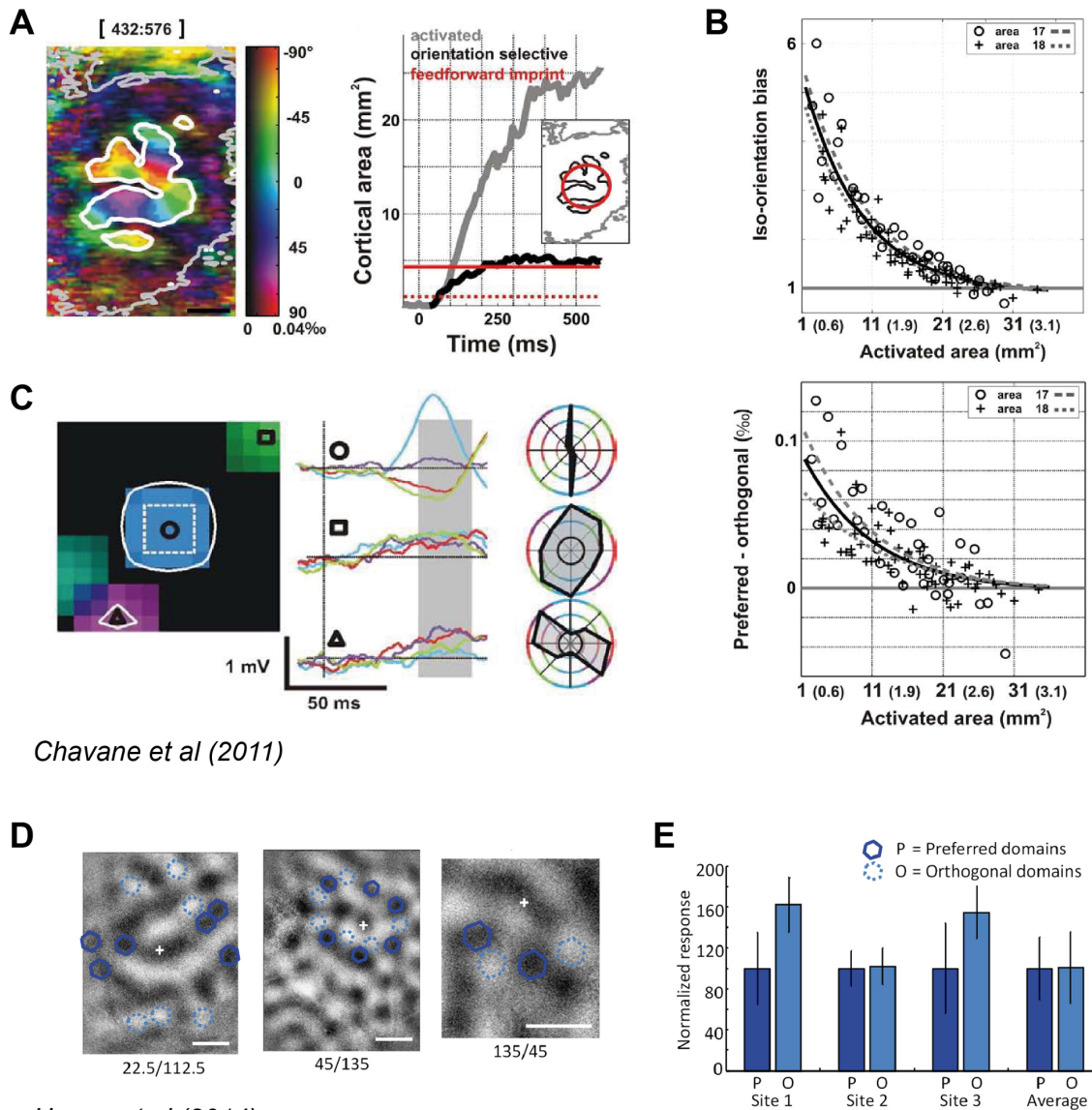
Here, we review more recent evidence for versatile connectivity rules reported in different species and with different recording techniques. Importantly, one should keep in mind that long-range horizontal axons only have a subthreshold influence on their postsynaptic targets (Bringuier et al. 1999). In order to study the selectivity of the postsynaptic target of these axons, it is therefore important to use methods that are sensitive to subthreshold membrane potential changes. Indeed, methods that only record spiking activity necessitate experimental protocols that co-activate the presynaptic source and postsynaptic target of the horizontal network, to study cross-correlation between neurons (Michalski et al. 1983; Ts'o et al. 1986; Schwarz and Bolz 1991; Das and Gilbert 1999). Under these conditions, it is hard to tease apart the direct effects of the horizontal axons rather than secondary activation of recurrent columnar circuits.

In 2011, Chavane and collaborators used complementary recording tools that specifically record the subthreshold activity of a mesoscopic population (voltage-sensitive dye imaging, VSDI), and of individual neurons (intracellular recordings) in area 17 and 18 of the anesthetized cat. The first method allowed us to visualize and quantify the orientation selectivity of the laterally spreading activity evoked by a local stimulus (Jancke et al. 2004). The second method enabled a precise measurement of the impact of this subthreshold spread of activity on individual neurons. Using VSDI in the cat area 17 and 18, the authors showed that a local oriented stimulus evokes a spread of activity along the horizontal dimension, extending up to three mm laterally (see also (Bringuier et al. 1999; Reynaud et al. 2012; Muller et al. 2014, 2018). It is to be noted that the spread of activity did not show any patchiness, contrary to the anatomical observations. However, we believe that this is to be expected considering the large variability in the patches that will be activated from different neurons, varying as a function of a neuron's

type, layer and position in the orientation map. As a consequence, and in sharp contrast to the extended horizontal activation, the orientation-selective component of this spread remains confined to the cortical feedforward imprint of the stimulus (Fig. 2A). The feedforward imprint being defined in Chavane et al (2011) as the population of neurons directly or partially activated by the feedforward stream. This effect was systematically observed in both areas 17 and 18 and quantified using complementary methods to quantify the decrease of the orientation selectivity with horizontal distance. Both at the level of orientation preference and orientation selective response, the bias towards like-to-like activation (and therefore functional connectivity) decreases exponentially with horizontal distance with a similar characteristic cortical space constant of about one mm or one hypercolumn (Fig. 2B). Importantly, this signifies, that, for a lateral radius of about 1.5 mm, the iso-orientation bias (Fig2B) was in the same range as that observed in the anatomy for similar lateral distance (Bosking et al. 1997, Kisvarday 1997; Schmidt et al. 1997; Malach et al., 1993, Rochefort et al., 2009). However, VSDI is a population measure of the subthreshold activation that pools activity from all neurons (excitatory and inhibitory), all compartments (dendrite, soma and axons) and mostly the upper layer (see Chemla et al 2017). Therefore, VSDI offers a unique population view of the functional activation but it is less precise than anatomical studies: it is for instance possible that the lack of overall bias comes from the mix of tuned and untuned subpopulations (see Kisvarday 2016 for further discussion). Chavane et al (2011) therefore used intracellular recordings to confirm the VSDI observations and further showed that this loss of orientation selectivity actually arises from the diversity of converging synaptic inputs originating from outside the classical RF (Fig. 2C). The conclusion from this work is that the lateral spread of cortical activity gradually loses its orientation iso-preference at a distance of around one hypercolumn and that there exists a range of strategies for different post-synaptic neurons.

In a more recent work, Huang et al (2014) provided similar and complementary results in a different species, V1 of the tree shrew, and using a different methodological approach. The authors used optical imaging of intrinsic signals to monitor the impact of intra-cortical optogenetic stimulation under various stimulation configurations. In particular, their results show that the optogenetic stimulation of excitatory neurons within a set of orientation domains in the cortex generated the same response amplitude for either iso- or orthogonal domain stimulation (Fig. 2D, E). The responses actually depended primarily on intra-cortical distance (similar to the results obtained via cross-correlation in (Das and Gilbert 1999). Using their innovative approach, the authors also tested stimulation along an axis in the retinotopic map, either collinear with the preferred orientation or orthogonal to it. The authors found no bias in either direction. Huang et al (2014) therefore provides independent and complementary evidence that the horizontal network, when probed with functional measures, does not show a bias for iso-orientation preference in V1. It should be noted however that using optogenetic stimulation of excitatory neurons may drive complex dynamical activation of the cortex (Li et al 2019), mixing excitatory and inhibitory recruitment of the lateral network with different dynamics. Since the authors have used intrinsic optical imaging, they could not access to the dynamics of the lateral activation that would be averaged out in the observed activation maps (see Kisvarday 2016 for further discussion).





Chavane et al (2011)

Huang et al (2014)

**Fig. 2 : Probing for the orientation selectivity of the horizontal network with functional imaging.** A-C Taken from Chavane et al (2011) and D-E from Huang et al (2014). **(A)** Voltage-Sensitive Dye Imaging of the orientation selective response evoked by local oriented gratings, example from area 17 of an anesthetized cat. (Left) Polar orientation map averaged over the final 145 ms of the response (time stamps indicated above the frame). Color hue and brightness code respectively for the preferred orientation and the strength of the orientation tuning. Contours delineate the outer border of the cortical domain within which significant activation level (thin gray contour) or significant orientation selective response (thick white contour) are observed. (Right) Spatial extent of the activated area (gray) and of its orientation-selective component (black) as a function of time. Red line indicates the expected limit of the feedforward imprint, defined and estimated from Albus (1975) as the population of neurons directly or partially activated by the feedforward stream. Dotted red line indicates the retinotopic area of the stimulus representation. Inset: The spatial extent of the activation spread (gray) and the orientation-selective

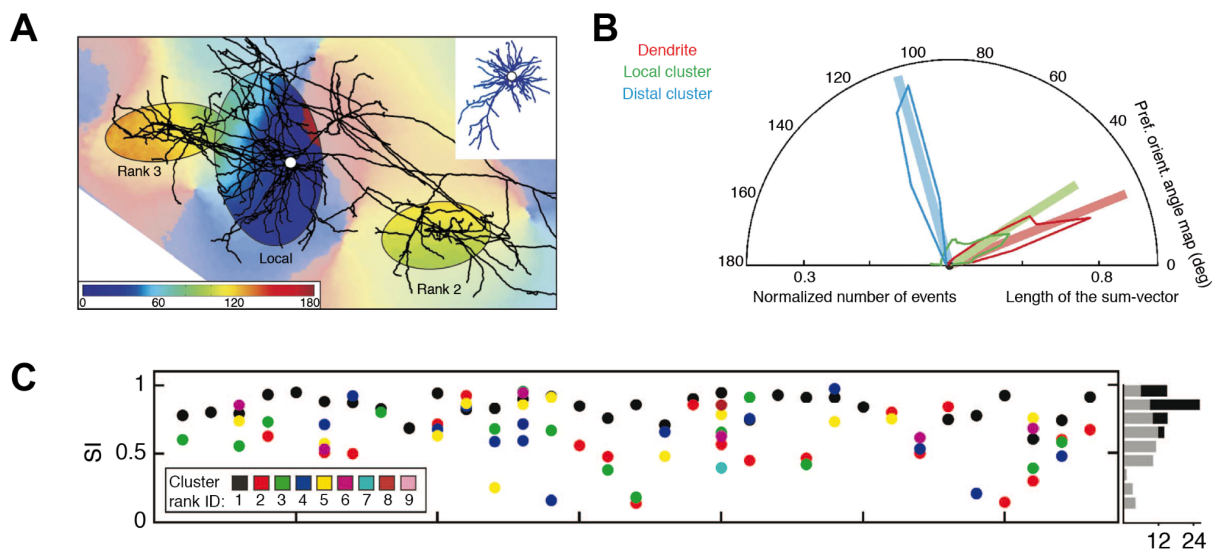


activation (black) are shown in comparison with the expected limit of the feedforward imprint (red). **(B)** Population analysis over nine hemispheres [three in area 17 (o) and six in area 18 (+)] of the horizontal distance-dependent decrease of orientation selectivity. (Top) Iso-orientation bias as a function of the spatial eccentricity of the lateral spread. The first point corresponds to the area of the initial cortical activation. Exponential fit is shown in black. (Bottom) Decrease in condition-wise modulation depth with lateral propagation distance. **(C)** Visuotopic orientation polar map of an intracellular subthreshold response; Color hue and brightness code respectively for the preferred orientation and the strength of the orientation tuning. The white contours delineate the significant responsive regions when combining both amplitude and orientation selectivity criteria. Middle: averaged subthreshold responses to four different orientations (same color code) presented for particular locations (circle, triangle, and square); scale bars: 50 ms and 1 mV; Right: normalized orientation-tuning curves, integrated within a fixed temporal window (shaded area of middle panel). The black circle indicates the spontaneous level for the depolarizing integral measure. **(D)** Three orientation maps measured with optical imaging of intrinsic signals (Huang et al 2014) with the extracellular recording site (white “+”). Optogenetic layout stimulation sites that were centered over orientation domains with the same orientation preference (blue solid hexagons) as the recording site (+), and stimulation sites that were centered over domains with the orthogonal preference (light blue dashed hexagons). Scale bars: 500  $\mu$ m **(E)** Extracellular responses to optogenetic stimulation of preferred domains (dark blue) and orthogonal domains (light blue) in the three example cases shown in D, and the average responses to stimulation of preferred or orthogonal domains across all cases examined ( $n = 10$ ).

## Anatomical measures

In a recent anatomical study, Martin et al (Martin et al. 2014) carefully re-evaluated the orientation bias of horizontal boutons from upper layer pyramidal neurons in cat area 17 using single cell intracellular labelling, optical imaging to reveal the orientation map, and advanced cluster-by-cluster analysis of synaptic boutons. In their analysis, Martin et al (2014) compared the distribution of the preferred orientations spanned by the neuron’s dendritic arbors (used to estimate the neuron’s preferred orientation) and the preferred orientation covered by axonal clusters of the neuron (Fig. 3A). In the example of Fig. 3A-B, the preferred orientation of the dendrite (red) matched the one of the local cluster (green) but not of the distal cluster (blue). Over 33 neurons, their results revealed a very large variability in the orientation selectivity of their distal clusters (colored in Fig. 3C), as estimated by their *Similarity Index* (1 corresponding to the same orientation preference distribution with respect to the neuron’s preferred orientation, 0 to an orthogonal orientation preference). Their results demonstrated the existence of a very large variance of SI (0.13-0.96) out of all 51 clusters they observed over the 25 neurons. To test whether the clusters positions within the orientation maps occur by chance, the authors made a detailed bootstrap statistical analysis of all 51 clusters, taking into account the bias that is introduced by the orientation map layout, the cluster size and position relative to the soma. Using this analysis, they found that a quarter of their clusters (14/51 clusters recently updated to 17/65, personal communication from Ruesch & Martin) were not positioned randomly in the map. Interestingly, only 9% (6/65) of these clusters (see their suppl Fig10I), had a significantly high SI, above the upper bound (hence iso-oriented), and 5% (3/65) below the lower bound (hence cross-oriented). In contrast 12% (8/65) were located in position of the orientation map unlikely to occur by chance while being neither iso nor cross-oriented with the labelled cell. As a

conclusion, only a weak minority of clusters (9%) are significantly tuned to iso-orientation from non-random position in the orientation map. Furthermore, as shown by Buzas et al (2006), this bias tends to decrease with lateral distance of the clusters, which is further in accordance with Chavane et al (2011). Finally, as observed in Huang et al (2014), Martin et al (2014) did not find any specific alignment of the cluster distributions in the retinotopic map that could favor collinear vs orthogonal interactions with the cell's preferred orientation. At a more macroscopic level, diversity was also shown from animal to animal in tree shrew V1, specifically in the fine orientation/retinotopic arrangement of extracellular anatomical labelling (i.e. a population of neurons). In their detailed analysis (Hunt et al. 2011), showed that there is a diversity of co-circular connectivity rules across animals, some showing a significant bias towards co-circular rules, some towards anti-circular rules, and others without biases. Thus, as stated by Martin et al (2014), the horizontal axons thus cannot be treated as an homogeneous network with a net iso-oriented bias, but rather should be described as strongly heterogeneous, an heterogeneity that may be a the core of its function (see also Kisvarday 2016).



*Martin et al (2014)*

**Fig. 3: Probing for the orientation selectivity of individual horizontal axons (from Martin et al 2014).** (A) Axon of an intracellularly labelled neuron is displayed over the orientation map. Ellipses show clusters of boutons (not shown) for local and more distal positions. Dendritic tree (inset) was colour coded by the orientation value of their corresponding pixels (soma ¼ white dot). Scale bar, 0.5 mm. (B) Radial plots of the normalized number of boutons counted in each local (green) and distal clusters (blue) but also the dendrite (red) for each preferred orientation (coloured curves). The individual vectors forming these hemispheric plots were summed up to generate one sum-vector (bold vector). The length of this sum-vector is termed as the 'tuning' of the dendrite or cluster. (C) Similarity Index (SI) values for individual clusters of 33 neurons sorted by normalized depth of soma. (Top) neurons (xaxis) can have clusters (colour coded by rank) with different SI (yaxis). The histogram on the right summarizes the SI across clusters of all neurons (grey=distal, black=local). Note the large variance within and across neurons.

## 274 COMPUTATIONAL MODEL LINKING STRUCTURE TO FUNCTION

275 Population measures and anatomical data constrain connectivity in cortical space, however the  
276 link between known anatomical details and the resulting functional expression (in terms of  
277 neural activity) is not obvious. Computational models provide a means to explore this  
278 relationship directly. Modelling studies of V1 consider a range of connectivity rules, and these  
279 frequently allow for the shaping of connection strengths based on the difference of orientation  
280 preference between connected sites. Abstracted models of single hypercolumns implement  
281 cross-orientation interactions in local circuits that further tune selectivity derived from weakly  
282 tuned LGN inputs (Ben-Yishai et al. 1995). Similar mechanisms for orientation selectivity in V1  
283 have been explored in models with recurrent, lateral connections over short distances (between  
284 neighbouring hypercolumns in L4) (Somers et al. 1995; Kang et al. 2003; Chariker et al. 2016).  
285 Connections that extend over many mm of cortex (i.e. across multiple pinwheels) are  
286 considered in visual cortex modelling studies of contextual modulation (Rubin et al. 2015),  
287 motion illusions (Rangan et al. 2005), geometric visual patterns (Bressloff et al. 2001; Baker and  
288 Cowan 2009; Carroll and Bressloff 2016), travelling waves (Bressloff and Carroll 2015), and in a  
289 general setting (Raizada and Grossberg 2003). Whilst models do commonly feature a decay  
290 (e.g. exponential or Gaussian) in the strength of orientation-based connections with distance  
291 (Goldberg et al. 2004; Blumenfeld et al. 2006), the tuning strength is not distance dependent,  
292 rarely systematically investigated and not constrained by anatomical data. The function of  
293 patchy long-range connections has further been investigated in contexts not specific to  
294 orientation encoding (Voges et al. 2010; Voges and Perrinet 2012). In general, long-range  
295 connections feature a strong iso-orientation bias motivated by long-held assumptions that do not  
296 take into account the more recent functional and anatomical studies that motivate a modification  
297 of this rule.

298 A common modelling choice for local excitation-inhibition connectivity is a so-called Mexican-hat  
299 with inhibition extending further than excitation (Marr and Hildreth 1980; Grossberg 1983;  
300 Somers et al. 1995; Bressloff et al. 2001). This choice is known to generate stable localised  
301 patterns of activity (rather than spatial unstable dynamics that spreads across cortex) (Laing  
302 and Troy 2003), however, excitatory connections in V1 can extend many mm further than the  
303 local inhibitory footprint. In general, models that also feature long-range excitation are used to  
304 study unbounded patterns of activity rather than localised responses to inputs (Bressloff et al.  
305 2001; Blumenfeld et al. 2006). (Rankin et al. 2014) extended the results of (Laing and Troy  
306 2003) to demonstrate that localised inputs can generate stable localised activity patterns (rather  
307 than spreading activity) with a connectivity rule (as suggested in (Buzás et al. 2001), and similar  
308 to Fig. 4A) that features long-range excitation, extending much further than the local inhibitory  
309 network.

310 (Rankin and Chavane 2017) developed a planar spatial model of orientation-selective activation  
311 in V1 L2/3 with the aim of bridging between known anatomical constraints on the tuning of long-  
312 range connections (Buzás et al. 2006) and the functional expression of laterally propagating  
313 activity driven by localised stimuli (Chavane et al. 2011). A neural field architecture with  
314 orientation-specific sub-populations provides a mesoscopic description of neural activity, ideal

for comparison with the temporal and spatial resolution in VSDI imaging experiments. A novel connectivity function was flexibly parametrized to investigate clustering of connections, their orientation bias and balance between excitation and inhibition. We adopted the non-orientation specific nature of local excitatory connections (Buzás et al. 2006) and inhibitory connections (Buzás et al. 2001); see also (Koch et al. 2016) for a discussion of orientation specificity of excitatory and inhibitory connections. Taking motivation from (Buzás et al. 2001), longer-range excitatory connections are proposed here to, although decaying with distance, form in rings at multiples of the hypercolumn separation  $L$  (Fig. 4A). This allows for the following important features to be captured: that excitatory connections 1) drop in number at a range of  $L/2$ , 2) have a peak at a range of  $L$  (and multiplies therefore) and 3) can extend several mm across cortex. Two parameters were tuned to agree with the available data from (Buzás et al. 2006), the width of peaks in number of excitatory connections (RW; two values shown in Fig. 4A) and their orientation bias (BR; illustrated in Fig. 4B-C).

We found a significant overlap between the anatomically relevant parameter range and patterns of cortical activation consistent with imaging experiments (Chavane et al. 2011). Hence, this computational approach allowed us to reconcile the imaging results with the reported level of orientation bias from anatomical studies. Specifically, (Chavane et al. 2011) found a sharp decay of orientation selective activation at the stimulus retinotopic footprint border, resulting in peripheral activation that was not orientation selective. Our results demonstrate that this sharp decay is contingent on three factors: the diffuse clustering of long-range connections, the intermediate range (consistent with anatomy) of their orientation bias and sufficient balance between excitation and inhibition. It is worth noting that orientation-biased long-range connections can recruit a local non-orientation-biased network at the target, resulting in non-orientation specific activation (Huang et al. 2014). The modelling work illustrates that the observed levels of orientation bias in anatomical studies actually predict long-range activation beyond the retinotopic stimulus footprint with a sharply decaying orientation selectivity profile.

The model offers further insights into the mechanistic value of excitatory-inhibitory balance, and of intermediate levels of orientation bias in long-range connections. Long-range excitatory connections (reaching much further than the lateral inhibitory profile) could easily lead to destabilization of activity generated by localised visual stimuli. Our model was used to show that if the orientation bias of lateral connections is excessively strong, or if inhibition is particularly weak, the network operates close to an instability leading to unbounded cortical activation. This provides another line of evidence in favour of distance-decaying orientation bias in lateral connections. Diversity of long-range connections increasing with distance (i.e. decreasing orientation bias with distance) reflects a potential need to activate a broader range of orientations as we move further from a local stimulus with a specific orientation. Furthermore, the fact that, under particular circumstances, the preferred orientation of the horizontal propagation may be at odds with the underlying orientation preference map could unravel some new unexpected computational capacities of the horizontal network, which may be present in visual areas beyond V1. For instance, the ability to link information across position and orientation for non co-circular filters, which is important for processing objects with sharp angles. In line with this hypothesis, (Chavane et al. 2011) showed that the spread of orientation

selective activity is not fixed but can increase with increasing spatial summation generated by annular stimuli.

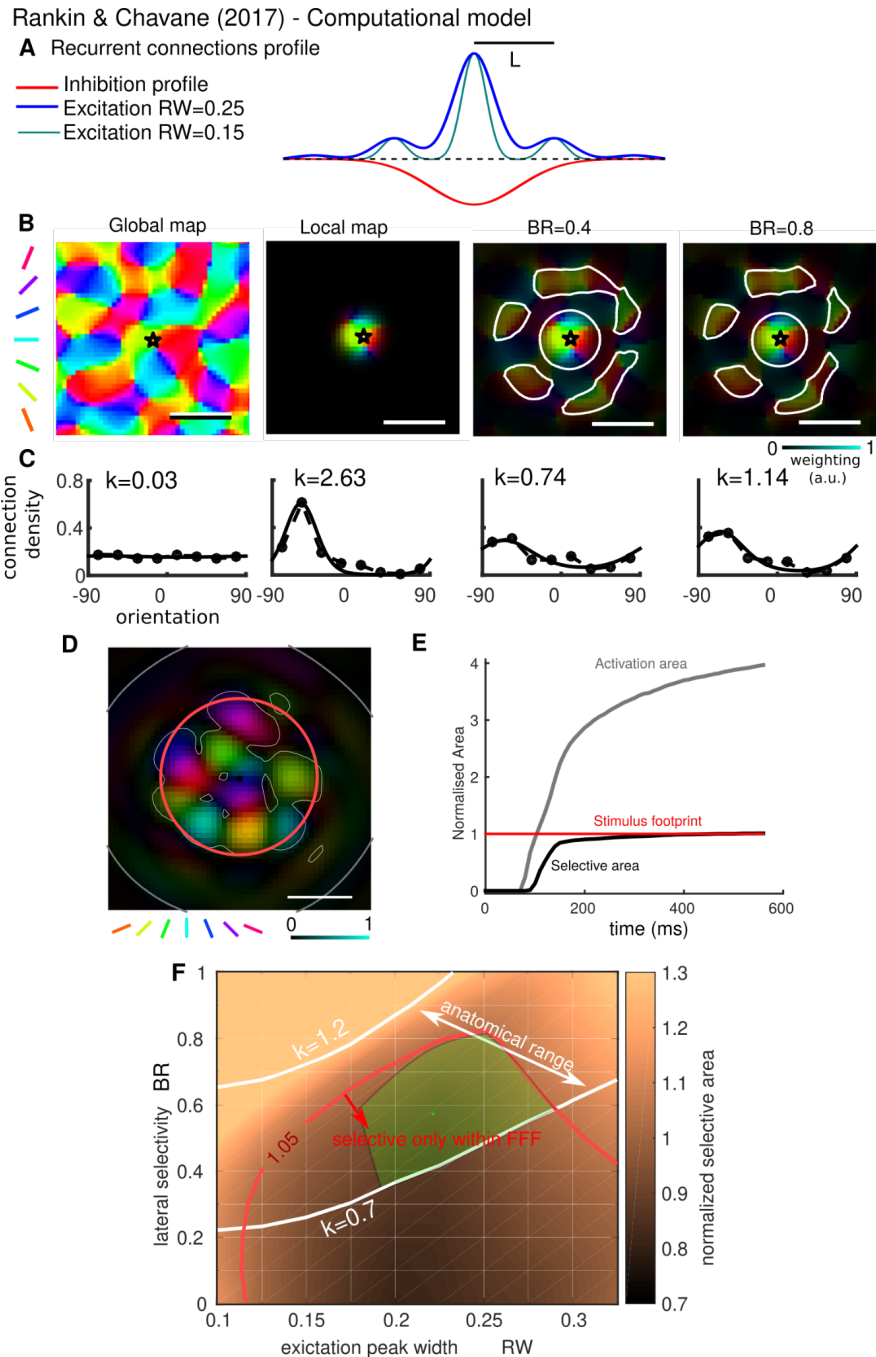


**Fig. 4: Neural field model to reconcile structure with function in primary visual cortex.** Definition of model connectivity with anatomical constraints (**A-C**) and illustration of model behaviour with operating region in agreement with functional characteristics (**D-F**). (**A**) Radial connectivity profile for inhibition (Gaussian decay) and excitation (locally Gaussian decay, longer range connections peak in number at distance  $L$  and multiples thereof). Ring width (RW) of peaks in excitatory connections illustrated for two

values. **(B)** Example of local preference map and resulting lateral connectivity for two values of the orientation bias of recurrent connections (BR). **(C)** Orientation tuning for each panel in **B** above (circles) with tuning parameter  $k$  from a best-fit von-Mises distribution (solid lines). Orientations are evenly represented in the global map but strongly biased at around  $-60^\circ$  for the local excitatory component (*local map*). The orientation bias of lateral connections increases to around  $k=1$  for  $BR>0.5$  (similar values reported in (Buzás et al. 2006)). **(D)** Model simulation snapshot at 600ms showing the orientation-selective component within a thin white contour, confined to the feedforward footprint FFF of the stimulus in red; the much broader non-orientation-specific activity falls within a grey contour extending beyond the plot limits. **(E)** Time history of the area within the non-orientation-specific contour and the orientation-selective contour. **(F)** Colour map across range of RW and BR values showing the selective area as in **D** normalised by FFF. Within the red contour the selective activation is constrained to the FFF. White contours show the anatomically constrained range for the connectivity parameters RW and BR where  $k=0.7-1.2$ . In the green region other constraints on the correct orientation and the radial decay rate of orientation selectivity are also satisfied (details in (Rankin and Chavane 2017)).

## FUNCTIONAL ADVANTAGES OF SUCH AN ORGANIZATION

The insights we have reviewed at the physiological and modeling levels support a range of novel hypotheses for the organization of long-range lateral connectivity in the primary visual cortex. A functional approach, asking "*why should neurons in V1 be connected laterally?*" provides a complementary perspective. Indeed, a major argument is that the structure of V1 should fulfill its function and implement principles of perceptual organization, such as the principle of *good continuation* to bring a contour's constituent edges together into a unified global percept (Wertheimer 1923). How might these principles connect knowledge across anatomy, physiology, theory, and modeling?

### *Principles of perceptual organization in natural images*

A major constraint for neurons in the primary visual cortex is that information is encoded locally in their activity and must be integrated globally across the visual field. Surprisingly, perceptual principles organizing the different fragments of an image can be directly extracted by analyzing a database of natural images. One such principle is that pairs of edges in natural images are most likely organized along aligned contours, and more generally on a common circle (Sigman et al. 2001); the authors extracted edges from natural images and estimated the orientation of each edge. For each pair of active edges, they showed that the angle of maximum interaction corresponds to a configuration for which they are close to co-circular. This long-range correlation is a marker of the structure of natural images and may provide strong prior knowledge for the perceptual organization of low-level features.

Such a structural prior can be described as a form of "association field" extending the concept of a neural receptive field to long-range local interactions. The seminal paper by Field (Field et al. 1993) defines the association field as the set of local oriented elements (edges) in the visual



field that facilitates the detection of a central oriented target. They showed that the association field obeyed a co-circular rule. In other words, if a common circle can pass through the central target and the peripheral element, they will facilitate each other's detection, and generate suppression otherwise. This association field is invariant to translations or rotations. It extends the prior of collinearity (like-to-like) or co-circularity (Sigman et al. 2001) to a more generic description of all possible co-occurrences. In particular, by exploring the interactions of edge pairs, they showed that these association fields explain the detection of paths embedded within a field of randomly oriented edges. The association field can then be understood in light of the computer vision problem of curve tracing. Parent and Zucker (1989) described it as a diffusion process over the tangent field of oriented edges, thus suggesting a principled and biologically realistic framework for association fields using long-range interactions.

This principle can be extended to explain psychophysical experiments in humans. Geisler et al. (2001) took a similar approach by reporting the full statistics of natural image edge co-occurrences. This yields a valuable model for the statistics of neighboring edges. First, the edges are organized into parallel textures favoring parallel edges, and second, there is a bias for co-circular edges (see Fig. 5A). Using a Bayesian approach, the authors derived a clustering scheme for chaining edges into contours that was confirmed by psychophysical experiments. This approach was later extended to the high-level cognitive problem of image categorization (Perrinet and Bednar 2015). The authors showed that using supervised learning, one could derive a scheme using the association field in that image to categorize whether it contains an animal. This simple model achieved similar performance to humans and to a deep hierarchical model (Serre et al. 2007). Surprisingly, the model made similar errors to humans. This illustrates first that association fields can be used to both group edges based on different tasks or to categorize images. This also shows that for the association field reflecting the statistics of edge co-occurrences in natural images, different datasets may lead to different association field structures (see Fig. 5A). As a consequence, it seems relevant at behavioral and ethological levels that mechanisms exist to tease apart the slight differences between the co-occurrence patterns present in different images, for instance the surprising patterns of a perfect co-circularity, or that of a pair of rare but informative orthogonal edges forming a T-junction. This would then explain part of the variability in the association fields which can be involved in visual integration processes.

### *How do these principles translate to the cortical space?*

As Geisler (2001) states, "*the obvious hypothesis for the local grouping is a neural population with the receptive field structure matched to the edge co-occurrence statistics*". Yet, the emergence of receptive field properties is a combination of anatomy and the dynamics of individual neurons. Can we link the statistics of natural images to the structure of processing in the primary visual cortex?

Olshausen and Field (1996) set out to show how the structure of V1 microcolumns can optimize

the efficiency of the neural representation for natural images. Hyvärinen and Hoyer (2001) extended this to include a regularization of the representation with cortical topography. Franciosi et al (2021) recently developed a biologically realistic, two-layered V1 sparse predictive coding model including pooling mechanisms to impose a neighborhood prior in cortical space, which includes by construction the possibility of representing as channels in each layer a variety of interaction patterns. Similarly, complex cells and topographic maps emerge, demonstrating the transfer of cortical connectivity in V1 to perceptual grouping principles. More surprisingly, depending on the density of neurons, different structures emerge to optimize cost efficiency: in addition to mammalian-specific features (such as topographical maps), a rodent-specific salt-and-pepper map emerges for models with a lower cell density. Interestingly, by focusing on this multi-channel convolutional architecture, the second layer showed a diversity of connectivities across channels, suggesting that differing anatomical constraints may induce different patterns of long-range lateral interactions.

A multi-layer sparse predictive coding model (Boutin et al 2020) allows for the influence of an extrastriate cortical area such as V2 on V1 to be modelled. The activity in the layers of this model emerge from the recurrent interactions between neurons within and across layers (rather than a feed-forward pass as in convolutional networks). Convergence to an efficient representation of edge filters and interaction maps (resembling association fields) emerges after several processing iterations. However, training on different natural image datasets can produce different interaction maps, in accordance with Perrinet and Bednar (2015). For example, training on images of human faces generated features resembling mouths or eyes, resulting in more sparse and longer range interactions. This suggests that instead of a simple similarity rule, lateral interactions between neurons reflect the variety of feature dependencies attached to the respective neurons. In addition, similarly to physiological observations (Gilbert and Li, 2013) we observed that the interaction becomes sharper with stronger feedback (see Fig. 5B), which proves a synergy between the different pieces of information encoded by the network, as illustrated by improved performance for denoising natural images.

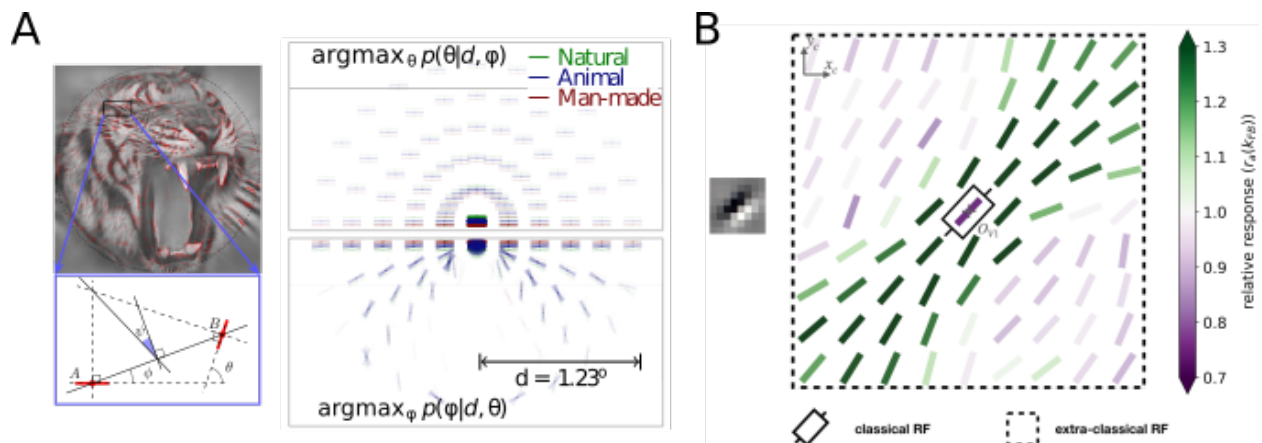


**Fig. 5: Function and diversity of Association Fields. (A)** Following the work of (Geisler et al. 2001), one could derive the association field from the statistics of natural images. This involves extracting edges from images (red segments) and computing for each pair the difference of angle  $\theta$  and the relative azimuth  $\phi$  of

one edge compared to the other. This allows to quantify the association field as the histogram, relative to a reference edge placed in the middle, for the most likely difference of angle - showing a prominent preference for parallel textures (top) or the relative azimuth, showing a prior for co-circular co-occurrences (bottom). The association field may vary for different databases with an excess of co-circularity in images containing animals, illustrating the variety of statistics faced by the visual system (Perrinet and Bednar 2015; modified with permission CC-BY). **(B)** Boutin et al (2020) describes a biologically realistic multi-layer model of the visual cortex. The model is shown natural images and is optimized to represent images in the most efficient way. Edge-like filters emerge (see an example in the inset) and we show here the interaction of this edge with other edges outside the range of its classical receptive field. This pattern shows a large facilitatory (green) or inhibitory (purple) effect relative to a model without feed-back. This functional modulation of the association field shows the importance of the activity in the whole network and we have further shown its shape could widely vary within the network and for different types of images, such as images of faces (Boutin et al 2020; modified with permission CC-BY).

### *Function and dynamics of long-range lateral interactions*

Overall, these theoretical models propose, as an alternative to the like-to-like structure, that there should be a wide variety of long-range lateral interaction patterns. It should be noted that most of the models described above deal with static natural images, whereas the visual world is characterized by a wealth of different dynamic scales, which raises the question of the role of neural dynamics in long-range lateral interactions.

If one imagines an edge moving in a direction parallel to its orientation, we can infer that we are following the tangent to a continuous contour. On the contrary, if the orientation of the edge is perpendicular to its direction, it is more likely that we are seeing a moving bar. This simple prototypical example shows that depending on the local intrinsic context, the optimal integration rule may change, as evidenced by intracellular recordings (Gerard-Mercier et al. 2016). If these interactions can be implemented via different contextual cues such as recurrent or feedback connections, it is also possible that the multidimensional representation of information on the cortical surface is much more than a simple topographical orientation map.

In addition, there is physiological evidence that association maps can be dynamically influenced by the task at hand. In (McManus et al. 2011), using a delayed-to-sample matching task, the authors trained monkeys to detect different patterns: a circle, a wiggle, or a line, which were embedded in a grid display of randomly oriented edges similar to that of (Field et al. 1993). They found that depending on the pattern being searched, the recorded association field adapted to preferentially exploit collinearities (for lines) or co-circularities (for circles). Such a differential processing raises an implementation problem for the unsupervised schemes described above. This problem could be solved in a supervised learning scheme (Perrinet and Bednar 2015) but raises the question of how this supervised credit is assigned in V1. A similar problem is inherent in the backpropagation rule in generic deep learning paradigms which can be solved in a predictive coding framework (Boutin et al. 2021).

Lastly, the anatomical connectivity may be patchy for different functions than just connecting like-to-like orientation patches. Indeed, patchy connections likely play an important role in

combining information from multiple visual cues beyond orientation, including context (Martin et al 2017). Indeed, modelling work has shown that patch-based connectivity increases the versatility of the dynamic repertoire of neural states (Voges et al, 2010). That work compared networks of realistic conductance-based neurons with a range of connectivity rules. These rules had different complexities, from a completely random connectivity, to a neighborhood-based local connectivity, and more interestingly, clustered networks including a patch-based connectivity rule. This was extended in a further modelling work (Voges and Perrinet, 2012) to include a comparison between a pure random patch-based connectivity and partially overlapping patches. As noted in (Kisvárdy 2016), these patch-based connectivity rules were sufficient to induce a large dynamic repertoire such as rhythms or travelling waves and was for instance characterized by enhanced variety in the shape of the power spectrum of population activity. In particular, such a range of dynamic behaviours is much richer when compared to those obtained with a random or local connectivity rule. Patchy connectivity rules introduce a heterogeneity in the lateral connections, which seems essential for building up an efficient population code (Martin et al 2014). In particular, this would allow the propagation of combinations of contextual cues which would reflect the richness of visual information in natural scenes.

To conclude this section, the function studied in these theoretical models hints at a solution using a superposition of different long-range connectivity profiles. The diversity of patterns and their adaptability to the task or statistics should overall improve processing efficiency in the primary visual cortex. Yet there remain open questions regarding the richness of these like-to-all patterns. Theories suggest potential strategies for addressing these open questions explicitly in neurophysiology, for example by synthesizing optimally responsive, model-driven dynamic stimuli (Walker et al. 2019).

## DISCUSSION

In this review, we have documented convergent evidence from physiology, anatomy and computational models that the orientation selectivity of horizontal network connectivity in the primary visual cortex of carnivores, ungulates and primates is more versatile than initially proposed, leading to the necessity to revisit the like-to-like connectivity rule (Mitchison & Crick 1982) still dominant today. At the anatomical level, there seems to be a diversity of connection rules between presynaptic source and postsynaptic target. At the individual cell level, anatomical studies have shown that the rule changes as a function of cell type (excitatory vs inhibitory) and layer/map locations (Yousef et al. 2001, Kisvárdy et al. 1994; Buzás et al. 2001, Yousef et al. 1999; Karube and Kisvarday 2010; Karube et al. 2017). Within one presynaptic origin, a large diversity exists with only moderate bias in the range of 1.5-2 times greater than chance (Bosking et al. 1997, Kisvarday 1997; Schmidt et al. 1997; Malach et al., 1993, Rochefort et al., 2009). More recent work by Martin et al (2014) on the upper layer pyramidal neurons of the cat V1 with a cluster-by-cluster analysis of horizontal boutons has shown the existence of a very large diversity from like-to-like, like-to-any, like-to-all and like-to-unlike connectivity rules. Altogether no net significative bias towards one of these rules could be observed in their bootstrap statistical analysis. Taken together, these anatomical results show

that there is diversity in the connectivity rules both within and between neuronal types and locations (see Kisvarday 2016 for an extensive review). At a more macroscopic level, it is interesting to note that Hunt et al (2011) also observed that the co-circularity rule is different from animal to animal.

When probed with functional measures of neuronal activity, in response to a local visual stimulus using techniques sensitive to subthreshold membrane potential fluctuations (Chavane et al 2011) or an optogenetic activation of specific orientation columns (Huang et al 2014), the diversity revealed in anatomical studies leads to the absence of net bias towards like-to-like interactions along the horizontal network (see Alonso & Kremkow 2014), but also the absence of patchy activation of the horizontal spread of activation. Importantly, VSDI measures demonstrate a clear exponential decay of the like-to-like connectivity bias with horizontal distance, an effect also observed in anatomy (Buzas et al 2006, Martin et al 2014). At short-range distances, similar iso-orientation biases, as reported in anatomical studies, were observed. However, after the equivalent of one hypercolumn, no significant bias could be observed (Chavane et al 2011).

All these papers therefore demonstrate the existence of a connectivity rule that links neurons in the primary visual cortex depending on their preferred orientation, neuronal type and position (layer and orientation map) and intra-cortical distance. This multidimensional connectivity rule is also subject to large diversity not just from neuron to neuron but also from animal to animal. Due to the difficulty in making predictions from this complex pattern, it is necessary to use computational approaches to probe for the expected functional behavior of such a network. In Rankin & Chavane (2017), we developed a neural-field model and demonstrated that the functional results observed in Chavane et al (2011) are indeed the expected mesoscopic behavior of such a network when its connectivity is constrained to match the orientation bias of connections from anatomy (Buzás et al. 2006), thus demonstrating that the functional observations are to be expected given our understanding of anatomical characteristics.

In this review, we wish to update the accepted like-to-like connectivity rule widely assumed as the building block for connecting a local neuronal network from one position in the visual field to its postsynaptic targets. The connectivity rule should be revised to a distance-dependent formulation: **from like-to-like bias at short horizontal distance to like-to-all at long horizontal distance (Fig. 1E)**. The space constant of the decrease of the like-to-like bias is about one hypercolumn distance. Functionally we can speculate that this translates to an iso-orientation bias for neurons with overlapping receptive fields and no net bias for neurons with non-overlapping receptive fields.

This may be at odds with the well-documented association field schema and co-circularity rules observed in natural scenes (Sigman et al. 2001, Geisler et al. 2001). However, it is important to differentiate the basic connectivity building block, that specifies unidirectional rules from a presynaptic region to a postsynaptic target, from lateral interactions, that are evoked by more complex stimuli that co-activate both presynaptic and postsynaptic regions (e.g., as in cross-correlation studies). The like-to-all long-distance connectivity rule can be seen as generic and

allows for a variety of interactions in the orientation and spatial domain. Importantly, this is possible if we take into account the large local diversity observed at neuronal level (Chavane et al 2011, Martin et al 2014, see also Monier et al 2003). Our proposition here is that such a rule could account for a wealth of interaction rules depending on the stimulus and/or the task. For instance, this would allow to account for the interactions necessary to process orientation discontinuities such as junctions or corners. Neurons in V1 have indeed been reported to be sensitive to orientation discontinuities, independent to the absolute orientation of the stimulus - set (Sillito et al. 1995, Jones et al 2001). This result could not be explained solely by iso-oriented lateral interactions. Such diversities could also contribute in shaping the orientation tuning of neurons away from primary orientation preference (i.e. horizontal and vertical orientations, Vidyasagar & Eysel 2015). More generally, using natural, stationary scenes and/or contour integration tasks may indeed favor association field interactions. However, depending on the type of natural images, Perrinet & Bednar (2015) have shown that these interactions may already differ significantly (see also Boutin et al. 2021). Moreover, dynamic non-stationary visual stimuli, such as a simple moving object, and tasks that rely on motion integration for instance, could lead to different associative rules for motion (Gerard-Mercier et al. 2016). In the case of integrating information along a coherent path for instance, visual information should be transported in the direction of motion (Perrinet and Masson, 2012) that can be in the cross-orientation dimension.

Importantly, co-circularity rules that link orientation and position with respect to a central oriented feature, are not found in the anatomy (Martin et al 2014, Hunt et al 2011), nor where they found by Huang et al (2014) using optogenetic stimulation of pattern in the horizontal network. This further supports a dynamic, context-dependent emergence of specific rules, such as co-circularity for contour integration in natural images, through higher-order network interactions. In that respect, Chavane et al (2011) observed that increasing the spatial summation of the stimulus increases the propagation of iso-orientation activity, even if the basic connectivity profile was shown to be not selective to orientation at long-range. This means that from a basic unselective building block, selective interaction can occur (for a proposition of possible mechanisms see Chavane et al (2011)). This effect could result from the fact that inhibitory neurons tend to make more horizontal connections with neurons with different orientation preference than excitatory neurons (Kisvárdy et al. 1994; Buzás et al. 2001). Increasing spatial summation could change the orientation-dependence of the excitatory/inhibitory balance and lead to the emergence of tuned activity at longer distance. More generally, the emergence of new selectivity depending on the stimulation pattern (or the task) is rendered possible by the existence of local diversity of orientation selective connections at neuronal level (Monier et al. 2003; Chavane et al. 2011; Martin et al. 2014). Therefore, different stimulation patterns will lead to activation of different recurrent subnetworks and the emergence of a variety of selectivity characteristics. It is indeed now well documented that non-trivial, paradoxical effects, can arise from recurrent balanced networks (Tsodyks et al. 1997; Ozeki et al. 2009; Pattadkal et al. 2018). In our model, we indeed observed that manipulating the balance between excitation and inhibition (i.e. reducing inhibition strength), predicts the emergence of spurious orientation selective activation through long-range lateral connections (Rankin & Chavane 2017).



Given the non-trivial effects that can arise with more complex stimuli, a number of avenues remain open to build on theoretical and modelling work. The model developed in (Rankin and Chavane 2017) could also be used to investigate selective recruitment and spatial summation in regions between localized oriented stimuli (Chavane et al. 2011; Huang et al. 2014). Indeed, increasing spatial summation increases the slope of selectivity decay at the stimulus boundary, whilst selective propagation reaches further across cortex, a property easily explored in the model by a more diverse class of localised stimuli. More generally, the model could be used to make predictions to decipher the selective functional connectivity rules that link position and orientation in cortical space. Importantly, it could also be extended to differentiate inhibitory cell subclasses as reported in (Buzás et al. 2001). As such it could generate functional predictions on e.g. the role of long-range basket cell connections that preferentially target cross orientations. Extending the framework further, a feature space including spatial frequency (SF) could be used to investigate lateral connections in light of recent work on interactions between orientation and spatial frequency maps (Romagnoni et al. 2015; Ribot et al. 2016).

In this review, we mostly focus on revisiting the connectivity rule of intra-cortical horizontal networks. However, it is important to consider that such connectivity patterns can also be influenced by feedback from higher cortical areas that provides a more diffuse and divergent input to the primary visual cortex (Salin et al., 1989, 1992). Anatomical studies in the cat, suggest that area 17 and area 18 cells are preferentially connected when they share similar preferred orientations (Gilbert and Wiesel, 1989). In the monkey, feedback from higher areas (V2 and V3) to V1 show variable level of patchiness (Stettler et al 2001; Angelucci et al 2002), unselective to orientation (Stettler et al 2001). In the cat, electrophysiological and inactivation studies of various downstream areas seems rather to influence only response amplitude or tuning width of neurons in area 17 of the cat (Martinez-Conde et al., 1999, Wang et al., 2000, 2007; Huang et al., 2004; Liang et al., 2007; Shen et al., 2008, Huang et al., 2007, Galuske et al., 2002; Shen et al., 2006). However, it is important to consider that feedback will interact with horizontal network as demonstrated in monkey visual cortex, with either specific interactions as suggested by CD Gilbert (Gilbert & Li 2013 for review), or contributing to center-surround processing (Hupé et al 1998, Roberts et al (2007) Poort et al 2012, Nurminen et al 2018).

In conclusion, we believe that there are enough arguments today to accept a change of connectivity rules for horizontal axons in V1, that is consistent with both new structural and new functional evidence. It remains to be established how this complex multidimensional rule (orientation x distance x neuron type x neuron location) is put into play out under different stimulus and task configurations. It would be important to understand what is the minimal stimulus design that can trigger particular tuned interactions for various spatial positions and whether it involves precisely the same neurons in the network. To test predictions that can arise from theoretical and computational approaches, new experimental tools to visualize large massive neural networks at neuronal level and sensitive to membrane potential fluctuations will be needed. Recent neuro-technological advances in awake animals, such as all-optical tools to measure and control a large set of neurons (Ju et al. 2018, Zhang et al. 2018), and the

development of new genetically-encoded voltage indicators that allow simultaneous two-photon microscopy subthreshold activity recording from many cells (Villette et al. 2019), provide the ideal experimental setting to probe the complex and dynamic network interactions underlying stimulus and task-dependent processing.

#### **Declarations**

Funding (information that explains whether and by whom the research was supported) : LP and FC are supported by CNRS and AMU and ANR “HorizontalV1” ANR-17-CE37-0006-02.

Conflicts of interest/Competing interests (include appropriate disclosures): The authors have no relevant financial or non-financial interests to disclose.

Availability of data and material (data transparency): Not applicable

Code availability (software application or custom code): Not applicable

Authors' contributions: All authors contributed equally to the review.

Additional declarations for articles in life science journals that report the results of studies involving humans and/or animals: Not applicable beca

#### **References:**

Alonso J-M, Kremkow J (2014a) Faculty Opinions recommendation of Optogenetic assessment of horizontal interactions in primary visual cortex. Faculty Opinions – Post-Publication Peer Review of the Biomedical Literature

Alonso J-M, Kremkow J (2014b) Faculty Opinions recommendation of Lateral Spread of Orientation Selectivity in V1 is Controlled by Intracortical Cooperativity. Faculty Opinions – Post-Publication Peer Review of the Biomedical Literature

Baker TI, Cowan JD (2009) Spontaneous pattern formation and pinning in the primary visual cortex. *J Physiol* 103:52–68

Ben-Yishai R, Bar-Or RL, Sompolinsky H (1995) Theory of orientation tuning in visual cortex. *Proceedings of the National Academy of Sciences* 92:3844

Blumenfeld B, Bibitchkov D, Tsodyks M (2006) Neural network model of the primary visual cortex: from functional architecture to lateral connectivity and back. *J Comput Neurosci* 20:219–241

Bosking WH, Zhang Y, Schofield B, Fitzpatrick D (1997) Orientation selectivity and the arrangement of horizontal connections in tree shrew striate cortex. *J Neurosci* 17:2112–2127

Boutin V, Franciosini A, Chavane F, et al (2021) Sparse deep predictive coding captures contour integration capabilities of the early visual system. *PLoS Comput Biol* 17:e1008629

Braitenberg V (1962) A note on myeloarchitectonics. *J Comp Neurol* 118:141–156

Bressloff PC, Carroll SR (2015) Laminar Neural Field Model of Laterally Propagating Waves of Orientation Selectivity. *PLoS Comput Biol* 11:e1004545

- 738 Bressloff PC, Cowan JD, Golubitsky M, et al (2001) Geometric visual hallucinations, Euclidean  
739 symmetry and the functional architecture of striate cortex. *Philos Trans R Soc Lond B Biol*  
740 *Sci* 356:299–330
- 741 Bringuier V, Chavane F, Glaeser L, Frégnac Y (1999) Horizontal propagation of visual activity in  
742 the synaptic integration field of area 17 neurons. *Science* 283:695–699
- 743 Buzás P, Eysel UT, Adorján P, Kisvárdy ZF (2001) Axonal topography of cortical basket cells  
744 in relation to orientation, direction, and ocular dominance maps. *J Comp Neurol* 437:259–  
745 285
- 746 Buzás P, Kovács K, Ferecskó AS, et al (2006) Model-based analysis of excitatory lateral  
747 connections in the visual cortex. *J Comp Neurol* 499:861–881
- 748 Carroll SR, Bressloff PC (2016) Phase equation for patterns of orientation selectivity in a neural  
749 field model of visual cortex. *SIAM J Appl Dyn Syst* 15:60–83
- 750 Chariker L, Shapley R, Young L-S (2016) Orientation Selectivity from Very Sparse LGN Inputs  
751 in a Comprehensive Model of Macaque V1 Cortex. *Journal of Neuroscience* 36:12368–  
752 12384
- 753 Chavane F, Sharon D, Jancke D, et al (2011) Lateral Spread of Orientation Selectivity in V1 is  
754 Controlled by Intracortical Cooperativity. *Front Syst Neurosci* 5:4
- 755 Chemla S, Muller L, Reynaud A, Takerkart S, Destexhe A, Chavane F. 2017. Improving voltage-  
756 sensitive dye imaging: with a little help from computational approaches. *Neurophotonics*  
757 4:031215. doi:10.1117/1.nph.4.3.031215
- 758 Creutzfeldt OD, Garey LJ, Kuroda R, Wolff JR (1977) The distribution of degenerating axons  
759 after small lesions in the intact and isolated visual cortex of the cat. *Exp Brain Res* 27:419–  
760 440
- 761 Das A, Gilbert CD (1999) Topography of contextual modulations mediated by short-range  
762 interactions in primary visual cortex. *Nature* 399:655–661
- 763 Douglas RJ, Martin KAC (2004) NEURONAL CIRCUITS OF THE NEOCORTEX. *Annual*  
764 *Review of Neuroscience* 27:419–451
- 765 Douglas RJ, Martin KA, Whitteridge D (1991) An intracellular analysis of the visual responses of  
766 neurones in cat visual cortex. *The Journal of Physiology* 440:659–696
- 767 Field DJ, Hayes A, Hess RF (1993) Contour integration by the human visual system: evidence  
768 for a local “association field.” *Vision Res* 33:173–193
- 769 Fisker RA, Garey LJ, Powell TP (1975) The intrinsic, association and commissural connections  
770 of area 17 on the visual cortex. *Philos Trans R Soc Lond B Biol Sci* 272:487–536
- 771 Geisler WS, Perry JS, Super BJ, Gallogly DP (2001) Edge co-occurrence in natural images  
772 predicts contour grouping performance. *Vision Res* 41:711–724
- 773 Gerard-Mercier F, Carelli PV, Pananceau M, et al (2016) Synaptic Correlates of Low-Level  
774 Perception in V1. *J Neurosci* 36:3925–3942

- 775 Gilbert CD, Wiesel TN (1979) Morphology and intracortical projections of functionally  
776 characterised neurones in the cat visual cortex. *Nature* 280:120–125
- 777 Gilbert CD, Wiesel TN (1989) Columnar specificity of intrinsic horizontal and corticocortical  
778 connections in cat visual cortex. *J Neurosci* 9:2432–2442
- 779 Goldberg JA, Rokni U, Sompolinsky H (2004) Patterns of ongoing activity and the functional  
780 architecture of the primary visual cortex. *Neuron* 42:489–500
- 781 Grossberg S (1983) The quantized geometry of visual space: The coherent computation of  
782 depth, form, and lightness. *Behav Brain Sci* 6:625–657
- 783 Huang X, Elyada YM, Bosking WH, et al (2014) Optogenetic assessment of horizontal  
784 interactions in primary visual cortex. *J Neurosci* 34:4976–4990
- 785 Hupé JM, James AC, Payne BR, Lomber SG, Girard P, Bullier J. 1998. Cortical feedback  
786 improves discrimination between figure and background by V1, V2 and V3 neurons. *Nature*  
787 **394**:784–787. doi:10.1038/29537
- 788 Hunt JJ, Bosking WH, Goodhill GJ (2011) Statistical structure of lateral connections in the  
789 primary visual cortex. *Neural Syst Circuits* 1:3
- 790 Jancke D, Chavane F, Naaman S, Grinvald A (2004) Imaging cortical correlates of illusion in  
791 early visual cortex. *Nature* 428:423–426
- 792 Jones HE, Grieve KL, Wang W, Sillito AM. 2001. Surround Suppression in Primate V1. *J*  
793 *Neurophysiol* 86:2011–2028. doi:10.1152/jn.2001.86.4.2011
- 794 Ju N, Jiang R, Macknik SL, et al (2018) Long-term all-optical interrogation of cortical neurons in  
795 awake-behaving nonhuman primates. *PLoS Biol* 16:e2005839
- 796 Kang K, Shelley M, Sompolinsky H (2003) Mexican hats and pinwheels in visual cortex.  
797 *Proceedings of the National Academy of Sciences* 100:2848–2853
- 798 Karube F, Kisvarday ZF (2010) Topographical organization of layer 4 and 6 spiny neurons over  
799 functional maps for visual signals in cat area 18. *Neuroscience Research* 68:e152
- 800 Karube F, Sári K, Kisvárdy ZF (2017) Axon topography of layer 6 spiny cells to orientation map  
801 in the primary visual cortex of the cat (area 18). *Brain Struct Funct* 222:1401–1426
- 802 Kaschube M, Schnabel M, Lowel S, Coppola DM, White LE, Wolf F. 2010. Universality in the  
803 Evolution of Orientation Columns in the Visual Cortex. *Science (New York, NY)* 1–5.  
804 doi:10.1126/science.1194869
- 805 Kisvarday Z (1997) Orientation-specific relationship between populations of excitatory and  
806 inhibitory lateral connections in the visual cortex of the cat. *Cerebral Cortex* 7:605–618
- 807 Kisvárdy ZF, Kim DS, Eysel UT, Bonhoeffer T (1994) Relationship between lateral inhibitory  
808 connections and the topography of the orientation map in cat visual cortex. *Eur J Neurosci*  
809 6:1619–1632
- 810 Koch E, Jin J, Alonso JM, Zaidi Q (2016) Functional implications of orientation maps in primary

- 811 visual cortex. *Nat Commun* 7:1–13
- 812 Laing CR, Troy WC (2003) PDE methods for nonlocal models. *SIAM J Appl Dyn Syst* 2:487–  
813 516
- 814 Markov NT, Misery P, Falchier A, et al (2011) Weight consistency specifies regularities of  
815 macaque cortical networks. *Cereb Cortex* 21:1254–1272
- 816 Marr D, Hildreth E (1980) Theory of edge detection. *Proc R Soc Lond B Biol Sci* 207:187–217
- 817 Martin KAC, Roth S, Rusch ES (2014) Superficial layer pyramidal cells communicate  
818 heterogeneously between multiple functional domains of cat primary visual cortex. *Nat*  
819 *Commun* 5:5252
- 820 Martin KAC, Roth S, Rusch ES. 2017. A biological blueprint for the axons of superficial layer  
821 pyramidal cells in cat primary visual cortex. *Brain Struct Funct* 222:3407–3430.
- 822 McManus JNJ, Li W, Gilbert CD (2011) Adaptive shape processing in primary visual cortex.  
823 *Proc Natl Acad Sci U S A* 108:9739–9746
- 824 Michalski A, Gerstein GL, Czarkowska J, Tarnecki R (1983) Interactions between cat striate  
825 cortex neurons. *Exp Brain Res* 51:97–107
- 826 Mitchison G, Crick F (1982) Long axons within the striate cortex: their distribution, orientation,  
827 and patterns of connection. *Proc Natl Acad Sci U S A* 79:3661–3665
- 828 Monier C, Chavane F, Baudot P, et al (2003) Orientation and direction selectivity of synaptic  
829 inputs in visual cortical neurons: a diversity of combinations produces spike tuning. *Neuron*  
830 37:663–680
- 831 Muller L, Chavane F, Reynolds J, Sejnowski TJ (2018) Cortical travelling waves: mechanisms  
832 and computational principles. *Nat Rev Neurosci* 19:255–268
- 833 Muller L, Reynaud A, Chavane F, Destexhe A (2014) The stimulus-evoked population response  
834 in visual cortex of awake monkey is a propagating wave. *Nat Commun* 5:3675
- 835 Nurminen L, Merlin S, Bijanzadeh M, Federer F, Angelucci A. 2018. Top-down feedback  
836 controls spatial summation and response amplitude in primate visual cortex. *Nature*  
837 *Communications* 1–13. doi:10.1038/s41467-018-04500-5
- 838 Ozeki H, Finn IM, Schaffer ES, et al (2009) Inhibitory stabilization of the cortical network  
839 underlies visual surround suppression. *Neuron* 62:578–592
- 840 Parent P, Zucker SW (1989) Trace inference, curvature consistency, and curve detection. *IEEE*  
841 *Transactions on Pattern Analysis and Machine Intelligence* 11:823–839
- 842 Pattadkal JJ, Mato G, van Vreeswijk C, et al (2018) Emergent Orientation Selectivity from  
843 Random Networks in Mouse Visual Cortex. *Cell Rep* 24:2042–2050.e6
- 844 Perrinet LU, Masson GS. 2012. Motion-Based Prediction Is Sufficient to Solve the Aperture  
845 Problem. *Neural Computation* 24:2726–2750. doi:10.1162/neco\_a\_00332

- 846 Perrinet LU, Bednar JA (2015) Edge co-occurrences can account for rapid categorization of  
847 natural versus animal images. *Sci Rep* 5:11400
- 848 Poort J, Raudies F, Wannig A, Lamme VAF, Neumann H, Roelfsema PR. 2012. The Role of  
849 Attention in Figure-Ground Segregation in Areas V1 and V4 of the Visual Cortex. *Neuron*  
850 **75**:143–156. doi:10.1016/j.neuron.2012.04.032
- 851
- 852 Raizada RDS, Grossberg S (2003) Towards a theory of the laminar architecture of cerebral  
853 cortex: computational clues from the visual system. *Cereb Cortex* 13:100–113
- 854 Rangan AV, Cai D, McLaughlin DW (2005) Modeling the spatiotemporal cortical activity  
855 associated with the line-motion illusion in primary visual cortex. *Proc Natl Acad Sci U S A*  
856 102:18793–18800
- 857 Rankin J, Avitabile D, Baladron J, et al (2014) Continuation of localized coherent structures in  
858 nonlocal neural field equations. *SIAM J Sci Comput* 36:B70–B93
- 859 Rankin J, Chavane F (2017) Neural field model to reconcile structure with function in primary  
860 visual cortex. *PLoS Comput Biol* 13:e1005821
- 861 Reynaud A, Masson GS, Chavane F (2012) Dynamics of local input normalization result from  
862 balanced short- and long-range intracortical interactions in area V1. *J Neurosci* 32:12558–  
863 12569
- 864 Ribot J, Romagnoni A, Milleret C, et al (2016) Pinwheel-dipole configuration in cat early visual  
865 cortex. *Neuroimage* 128:63–73
- 866 Roberts M, Delicato LS, Herrero J, Gieselmann MA, Thiele A. 2007. Attention alters spatial  
867 integration in macaque V1 in an eccentricity-dependent manner. *Nat Neurosci* 10:1483–  
868 1491.
- 869 Rockland KS, Lund JS, Humphrey AL (1982) Anatomical binding of intrinsic connections in  
870 striate cortex of tree shrews (*Tupaia glis*). *J Comp Neurol* 209:41–58
- 871 Romagnoni A, Ribot J, Bennequin D, Touboul J (2015) Parsimony, Exhaustivity and Balanced  
872 Detection in Neocortex. *PLoS Comput Biol* 11:e1004623
- 873 Rubin DB, Van Hooser SD, Miller KD (2015) The stabilized supralinear network: a unifying  
874 circuit motif underlying multi-input integration in sensory cortex. *Neuron* 85:402–417
- 875 Sarti A, Citti G, Petitot J (2008) The symplectic structure of the primary visual cortex. *Biol*  
876 *Cybern* 98:33–48
- 877 Schmidt KE, Kim DS, Singer W, et al (1997) Functional specificity of long-range intrinsic and  
878 interhemispheric connections in the visual cortex of strabismic cats. *J Neurosci* 17:5480–  
879 5492
- 880 Schwarz C, Bolz J (1991) Functional specificity of a long-range horizontal connection in cat  
881 visual cortex: a cross-correlation study. *J Neurosci* 11:2995–3007



- 882 Serre T, Oliva A, Poggio T (2007) A feedforward architecture accounts for rapid categorization.  
883 Proc Natl Acad Sci U S A 104:6424–6429
- 884 Sigman M, Cecchi GA, Gilbert CD, Magnasco MO (2001) On a common circle: natural scenes  
885 and Gestalt rules. Proc Natl Acad Sci U S A 98:1935–1940
- 886 Sillito AM, Grieve KL, Jones HE, et al (1995) Visual cortical mechanisms detecting focal  
887 orientation discontinuities. Nature 378:492–496
- 888 Somers DC, Nelson SB, Sur M (1995) An Emergent Model of Visual Cortical Orientation  
889 Selectivity in cat visual cortical simple cells. The Journal of Neuroscience 15:5448–5465
- 890 Ts'o DY, Gilbert CD, Wiesel TN (1986) Relationships between horizontal interactions and  
891 functional architecture in cat striate cortex as revealed by cross-correlation analysis. J  
892 Neurosci 6:1160–1170
- 893 Tsodyks MV, Skaggs WE, Sejnowski TJ, McNaughton BL (1997) Paradoxical effects of external  
894 modulation of inhibitory interneurons. J Neurosci 17:4382–4388
- 895 Vidyasagar TR, Eysel UT. 2015. Origins of feature selectivities and maps in the mammalian  
896 primary visual cortex. *Trends in Neurosciences* 38:475–485. doi:10.1016/j.tins.2015.06.003
- 897 Villette V, Chavarha M, Dimov IK, et al (2019) Ultrafast Two-Photon Imaging of a High-Gain  
898 Voltage Indicator in Awake Behaving Mice. Cell 179:1590–1608.e23
- 899 Voges N, Guijarro C, Aertsen A, Rotter S (2010) Models of cortical networks with long-range  
900 patchy projections. J Comput Neurosci 28:137–154
- 901 Voges N, Perrinet L (2012) Complex dynamics in recurrent cortical networks based on spatially  
902 realistic connectivities. Front Comput Neurosci 6:
- 903 Walker EY, Sinz FH, Cobos E, et al (2019) Inception loops discover what excites neurons most  
904 using deep predictive models. Nat Neurosci 22:2060–2065
- 905 Wertheimer M (1923) Untersuchungen zur Lehre von der Gestalt. II. Psychologische Forschung  
906 4:301–350
- 907 Yousef T, Bonhoeffer T, Kim DS, et al (1999) Orientation topography of layer 4 lateral networks  
908 revealed by optical imaging in cat visual cortex (area 18). Eur J Neurosci 11:4291–4308
- 909 Yousef T, Tóth E, Rausch M, et al (2001) Topography of orientation centre connections in the  
910 primary visual cortex of the cat. Neuroreport 12:1693–1699
- 911 Zhang Z, Russell LE, Packer AM, et al (2018) Closed-loop all-optical interrogation of neural  
912 circuits in vivo. Nat Methods 15:1037–1040
- 913